Electronic Supplementary Information for Journal of Materials Chemistry C

Chiro-optical response in helically arranged achiral dielectric nanoparticles

Haobijam Johnson Singh[a,*] and Ambarish Ghosh[a,b,c,**]

[a] Department of Physics, Indian Institute of Science, Bangalore, 560012

[b] Centre for Nano Science and Engineering, Indian Institute of Science, Bangalore, 560012

[c] Department of Electrical Communications Engineering, Indian Institute of Science, Bangalore 560012, India

* johnsonthonga196@gmail.com

** ambarish@ iisc.ac.in

Table of Contents

Supplementary Figures:

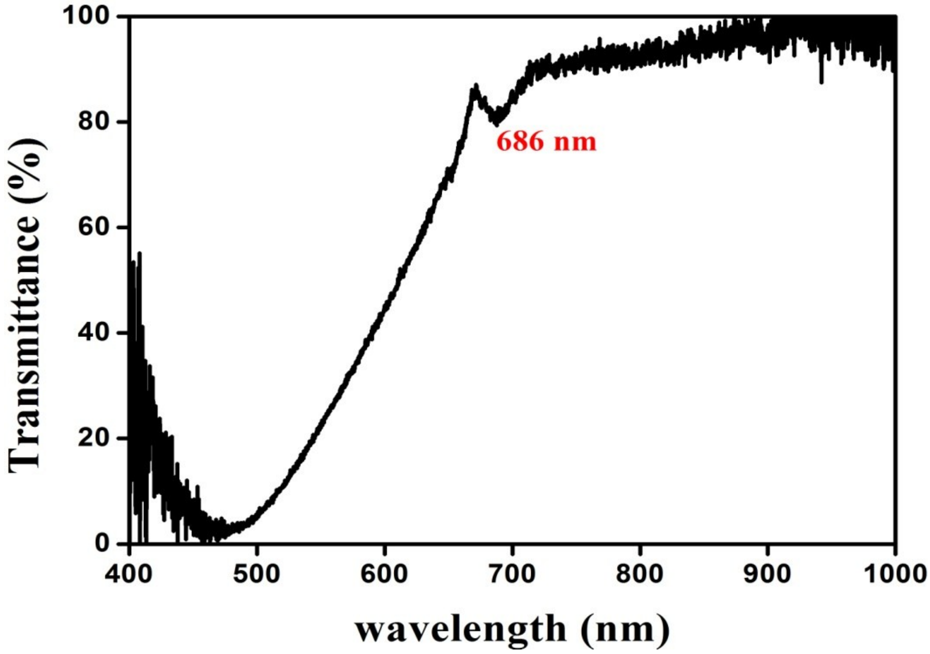

Fig. S1: Measured transmittance spectra of pattern photoresist pillars on a glass substrate. A plane glass slide was used as the reference sample.

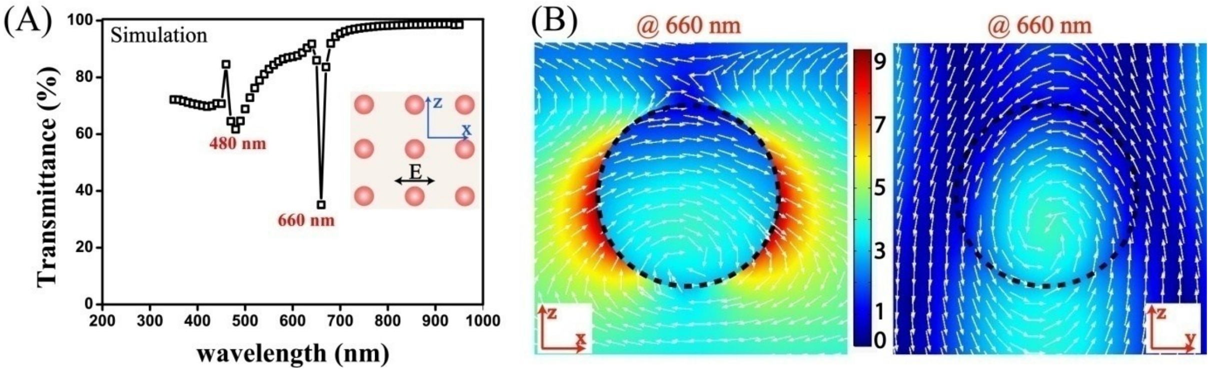

Fig. S2: (A) Simulated transmittance spectra for a 2D square aSi nanoparticle array showing a collective lattice mode at 660 nm in addition to single particle resonance at 480 nm. (B) False colour plot of norm of electric field enhancement ($\|\mathbf{E}/\mathbf{E_0}\|$) at 660 nm at zx and yz plane for incident linearly polarised light along x axis. Arrows (white colour) indicate direction of **E** vector in zx plane and **H** vector in yz plane. A circular distribution of **H** vector in yz plane within the particle confirms the electrical dipolar nature of this resonance. Experimentally (ellipsometry) determined optical constant values were used in the calculation.

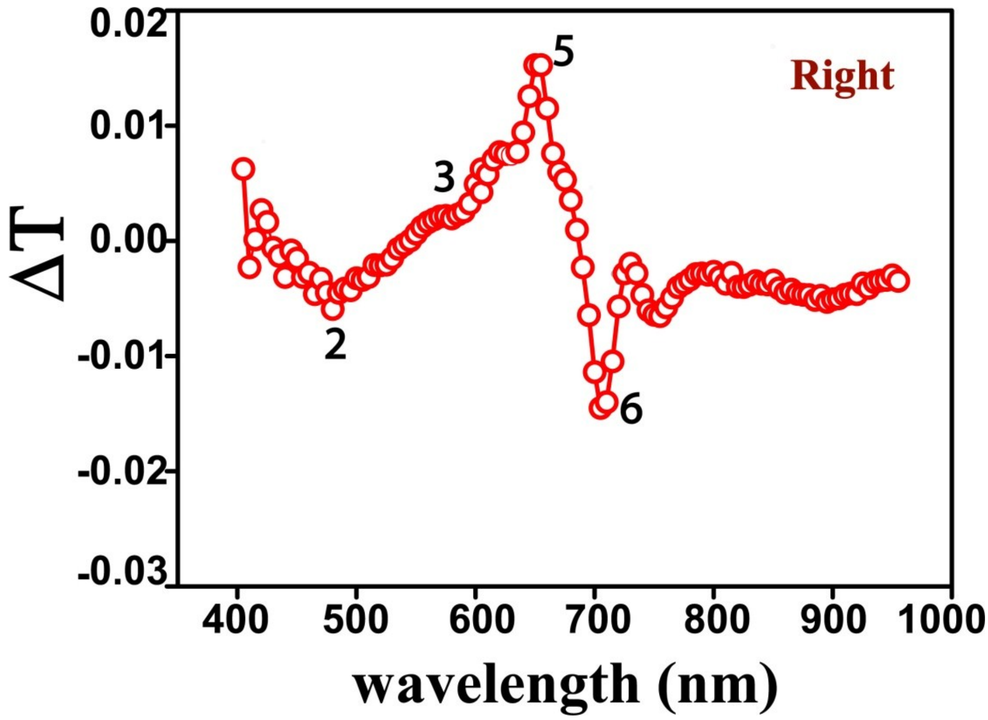

Fig. S3: Measured chiro-optical response in the form of circular differential transmittance, ΔT for right handed sample. The CD bands are marked by numerical numbers.

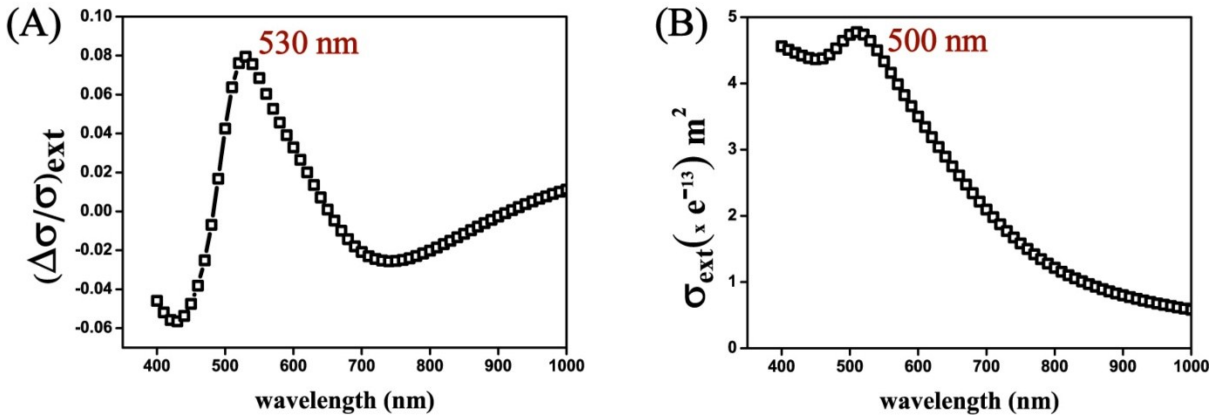

Fig. S4: (A) Simulated anisotropy factor response of 4 aSi nanoparticles arranged along a helix (B) Corresponding extinction cross section spectra of the system. Experimentally (ellipsometry) determined optical constant values were used in the calculation.

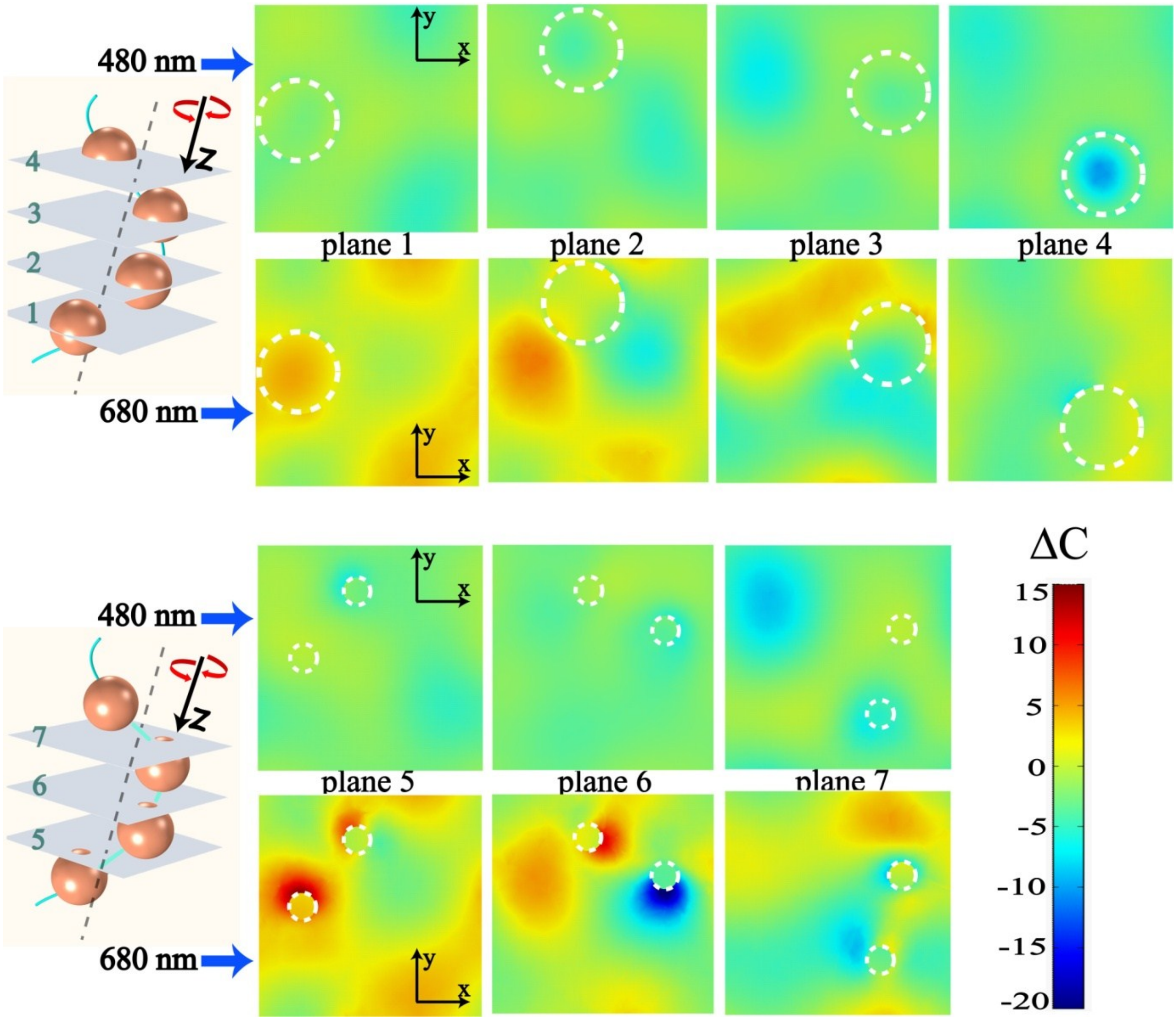

Fig. S5: False colour plot of the chirality enhancement parameter, ΔC at different planes perpendicular to the helix axis (schematics shown) corresponding to 480 nm and 680 nm resonance modes. ΔC at 680 nm is strongly enhanced in comparison to 480 nm and maximum value were found in between nanoparticle gaps. White dotted lines depict the contour of the nanoparticles intersecting with the planes.

Optical chirality is defined as $C(\vec{r}) = -\frac{\epsilon_0 w}{2} Im\left[\vec{E}^*(r).\vec{B}(r)\right]_1$, where $\vec{E}(r)$and $\vec{B}(r)$refer to the complex field amplitudes, and w is the frequency of the EM wave. The circular differential rate of excitation of a chiral molecule present at a position $\vec{r}$ is proportional to $\Delta C = (C^+(\vec{r}) - C^-(\vec{r}))/|C^{CPL}(\vec{r})|$ [1], where +/- refers to left and right circular polarization states of the incident wave respectively, and $C^{CPL}(\vec{r})$ refers to the optical chirality of the field in the absence of the nanostructure.

Supplementary Discussion:

I. Methods Section:

1. Sample Fabrication:

Fabrication of dielectric nanoparticle array system consists of two steps. First a 2D square array of pattern photoresist (PR) is fabricated on a glass substrate using laser interference lithography[2] technique. The pattern substrate was then used as a seed layer during Glancing angle deposition[3] of dielectric material.

Laser Interference Lithography (LIL)[2]: We used LIL (Laser Interference Lithography) in Lloyd's mirror configuration where a 356 nm laser line was used to create a 2D square array pattern. This was subsequently used as a seed layer for GLAD. The substrates (glass slides) are first cleaned chemically with piranha solution (mixture of H_2SO_4 and H_2O_2 in 3:1 ratio) to remove native oxide and then dehydrated at 250°C on a hot plate for 10 mins to remove any moisture content on the substrates. Once the substrates are cooled downed to room temperature a layer of positive photoresist (PR) (Shipley, 1805) is spin coated at 4000 rpm for about 40 seconds giving a film thickness of about 400 nm. The PR coated substrates are then prebake at 110°C on a hot plate for about a minute. Following this the substrates are exposed under the LIL (laser interference lithography) set up with an average dose of 300 mJ/cm^2 and later developed in MF26A developer (AZ EM electronics). Double exposure technique with 90° substrate rotation was adopted which resulted in 2D square array patterns.

Glancing Angle Deposition (GLAD)[3]: The LIL pattern substrate was used as a seed layer during the deposition of dielectric material which is carried out in a physical vapour deposition chamber equipped with an e-beam source. The pattern glass substrate was placed at an extreme angle (≥ 84°) to the source of incoming vapour and was rotated (clockwise or counter clockwise) at a speed of 0.05 – 0.1 rpm for chiral geometry and a speed of 0.15 – 0.3 rpm for the achiral geometry. In both the cases the deposition rate was maintained around 0.2 – 0.3 nm/second and the pressure was kept less than 6 $\times 10^{-6}$ mbar. Silicon and MgF_2 were alternately evaporated as required to create dielectric nanoparticle array systems.

1. ***Characterization:***

Scanning Electron Microscopy (SEM): The samples were first characterised using an ultra high resolution scanning electron microscopy (GEMINI, Zeiss) to confirm the proposed structure as well as the geometrical parameters of the helically arranged Si nanoparticles. The parameters are listed as:

Helix pitch (vertical) ~ 1 μm; Helix radius ~ 200 nm;

Nanoparticle size ~ 250 nm; Particle to particle spacing ~ 400 nm

In-plane lattice spacing ~ 650 nm

Photoresist pillar (seed layer) Height ~ 500 nm

Transmittance: The transmittance measurement of the dielectric nanoparticle array systems were carried out using an optical fiber based UV-VIS spectrometer (Ocean Optics USB 4000). The light beam emitted from the fibre was first collimated which was then polarised after passing through a Glan-Taylor polarizer. The polarised light was then allowed to incident on the sample normally. The transmitted light was then collecting using a collecting lens and integrated for 30 ms and then finally sent to the USB spectrometer. A glass substrate spin coated with photoresist was used as the reference sample.

Circular Dichroism: The chiral films were optically characterized in a system comprising of a lamp and a monochromator (Horiba Yvon), photoelastic modulator (Hinds Instruments) and photodiode (Thorlabs). Light of a particular wavelength was modulated between left and right circularly polarized states at 50 KHz and transmitted through the substrate onto the photodetector. The length of the cables and the load resistance across the photodiode was kept sufficiently low to ensure the temporal response of the detector to be faster than 150 KHz. The circular dichroism signal was measured though a lock-in amplifier (Signal Recovery) through standard phase locked detection techniques. The absolute transmittance of the samples was measured using UV-VIS spectrometer (Ocean Optics).

Ellipsometry: Ellipsometry measurements were carried out using Woollam Ellipsometer equipped with Deuterium and Quartz Tungsten Halogen lamp capable of scanning from 245 nm all the way to 1000 nm wavelength. A thin film of a-Si deposited by e beam evaporator both on cleaned silicon wafer as well cleaned glass slide were used for the measurements.

II. Numerical Simulations:

Numerical simulations were carried out using Comsol Multiphysics 5[4], a FEM (finite element method) based numerical software to calculate the circular differential response of the core-shell helical nanostructures. We adopted full field formalism with periodic boundary conditions (Floquet) applied on all the four sides of the computational geometry assuming an infinite 2D periodic structure in the x-y plane. The aSi nanoparticles were assumed to be spheres and he incident beam was assumed to be circularly polarised light (linearly polarised, LPL for the achiral 2D nanoparticle array) propagating along the helix axis in the z direction. The particles were positioned at the centre of the computational window without a semi-infinite substrate and assumed to be embedded in air medium (ε_m = 1.0). The frequency dependent complex dielectric function values for silicon used in the simulations were experimentally (ellipsometry) determined. Direct solver method was adopted to solve for the wave equation both for RCP and LCP (as well as for LPL incident light) and the transmittance was extracted using S-parameters which were further used for calculating circular differential transmittance. Sweep parameter was used to scan the wavelength range from 400 nm to 1100 nm.

For calculating single particle response scattered field formalism was adopted. We used a spherical PML of thickness 200 nm and order 1 surrounding the model geometry. The PML was placed at half-wavelength away from the NPs. The entire structure was divided into domains and sub-domains, and each domain was meshed using free tetrahedral meshing of maximum element size 6 elements per wavelength outside the dielectric nanoparticle. We adopt iterative solver to solve the wave equation, such as to calculate the extinction cross sections for LCP, RCP and LCP incident lights. Sweep parameter was used to scan the wavelength range from 400 nm to 850 nm. From the calculated cross sections for LCP and RCP, anisotropy factor 'g' was calculated using[5]

$$g = \frac{\sigma_{CD}}{\sigma_{avg}}$$

where $\sigma_{CD} = \sigma_L - \sigma_R$ and $\sigma_{avg} = (\sigma_L + \sigma_R)/2$

Simulation Parameters:

For the results shown in Figure 3 of the main manuscript:

Nanoparticle shape: Sphere; Radius: 115 nm; center to center spacing: 332 nm; lattice periodicity: 650nm; Helix radius = 200 nm; Helix pitch = 1 µm.

For the results shown in Fig.S2 of the supplementary information:

Nanoparticle shape: Sphere; Radius: 115 nm; lattice periodicity: 650nm.

References:

1. Y. Tang and A. E. Cohen, *Phys.Rev.Lett.* 2010, **104**, 163901.
2. S. Brueck, *Proceedings of the IEEE* 2005, ***93*** **(10)**, 1704-1721.
3. M. M. Hawkeye and M. J. Brett, *Journal of Vacuum Science & Technology A: Vacuum, Surfaces, and Films* 2007, **25 (5)**, 1317-1335.
4. Comsol Multiphysics, Version 5.0, 2014.
5. Z. Fan and A. O. Govorov, *Nano letters* 2010, **10 (7)**, 2580-2587.